Electronic Supplementary Material (ESI) for Journal of Materials Chemistry A.

Electronic Supplementary Information

Efficient and stable electroreduction of CO_2 to CH_4 on CuS nanosheet arrays

Zhe Zhao, Xianyun Peng, Xijun Liu, Xiaoming Sun, Jing Shi, Lili Han, Guoliang Li and Jun Luo

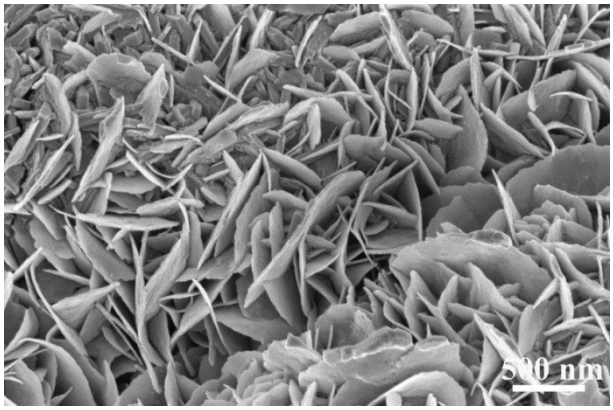

Figure S1 SEM of the precursor.

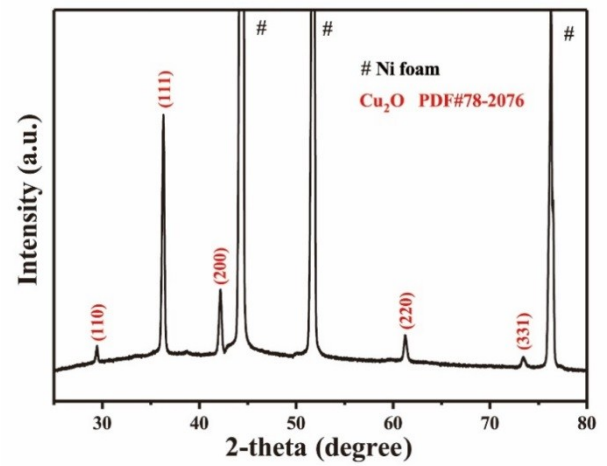

Figure S2 XRD pattern of the precursor.

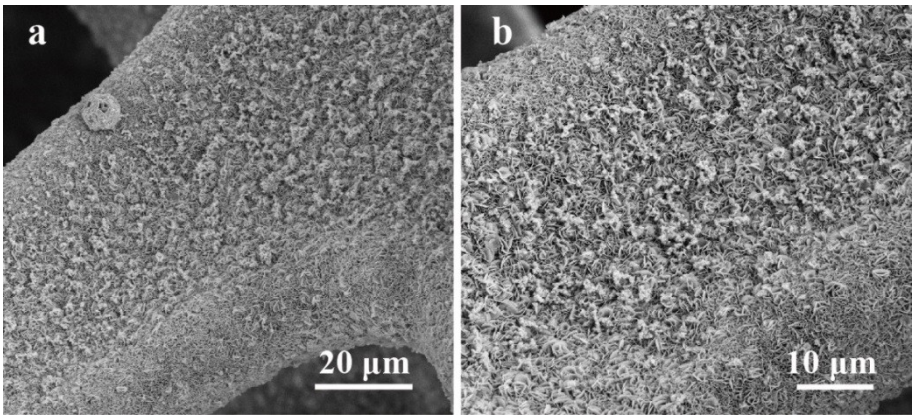

Figure S3 SEM image of CuS@NF.

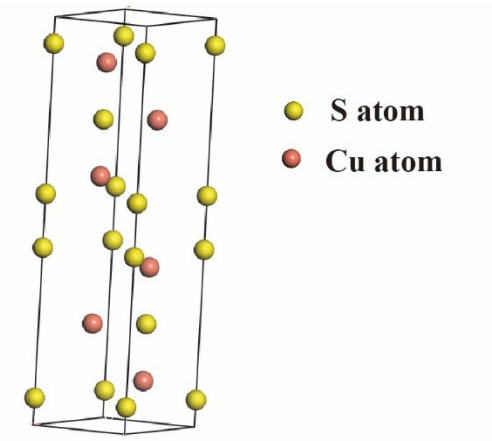

Figure S4 The atom structure model of CuS crystal.

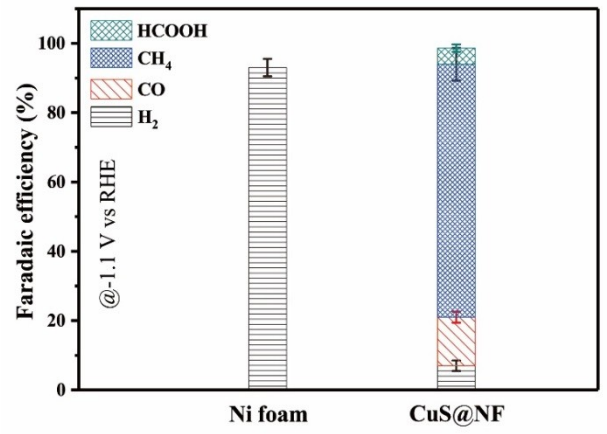

Figure S5 Faradic efficiency for different products.

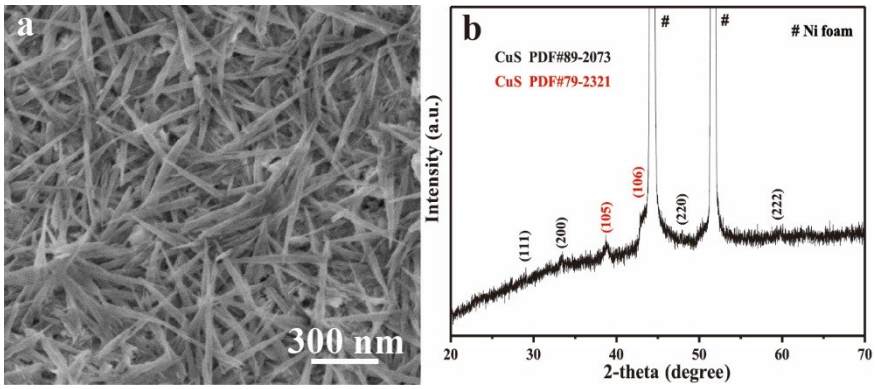

Figure S6 CuS nanowire arrays grown on the surface of a nickel foam, denoted as CuS-NW@NF. (a) SEM image; (b) XRD pattern.

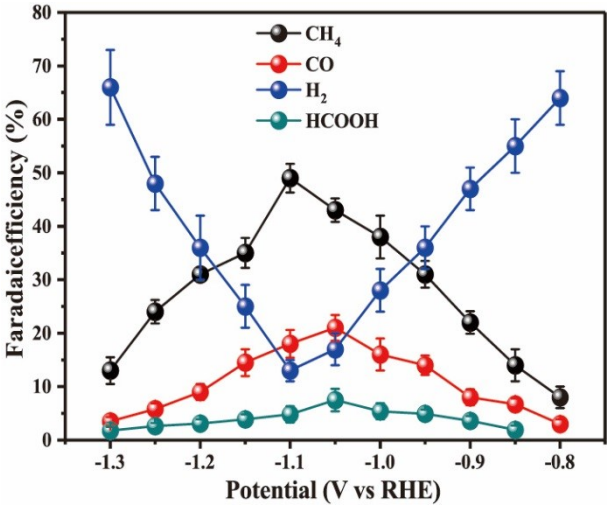

Figure S7 Faradaic efficiencies of CuS-NW@NF for CH_4, CO, H_2 and HCOOH at various applied potentials.

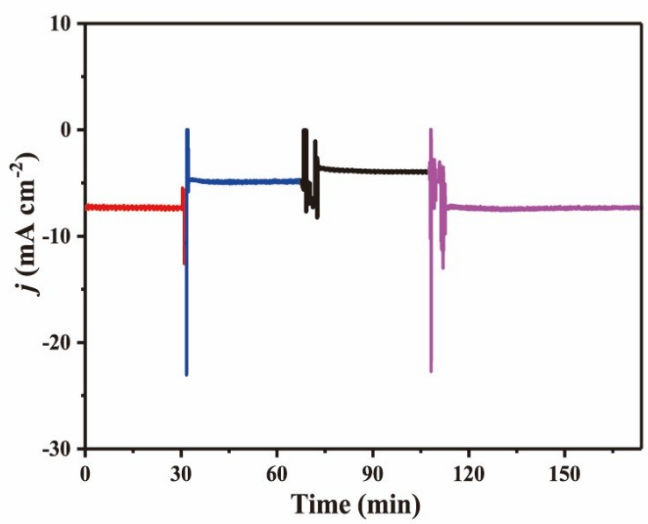

Figure S8 Current density (*j*) vs. time at −1.1 V in CO_2-saturated $KHCO_3$ solutions. This experiment and its result are similar to those in ref 41: After the first 30-min electroreduction with a stable current density of 7.32 mA cm^{-2} in a 0.5 M CO_2-saturated $KHCO_3$ solution (the red trace), the CuS@NF electrode was pulled out, rinsed quickly with a fresh 0.5 M $KHCO_3$ solution and immersed into another fresh 0.5 M CO_2-saturated $KHCO_3$ solution. Electroreduction was then conducted again for 30 min (the blue trace). The same procedure was repeated one more time (the black trace). In each of the blue and the black traces, an obvious decrease in the current density was observed. This decrease is because that in the red trace, the CuS phases on the electrode were partially reduced to metallic Cu, releasing some S species into the corresponding solution in order to maintain the (electro)chemical reaction equilibrium. Consequently, in the blue trace, when a fresh CO_2-saturated $KHCO_3$ solution was used, the S^{2-} content in the Cu/CuS electrode was lower than that in the red trace, causing a lower current density. The black trace has the same case. After the black trace, the same procedure was repeated, except that 1 mM K_2S was added into the corresponding $KHCO_3$ solution (the purple trace). Thus, the current density recovered to the initial value and remained constant, indicating the important role of S^{2-}

in the CO_2 electroreduction on CuS.

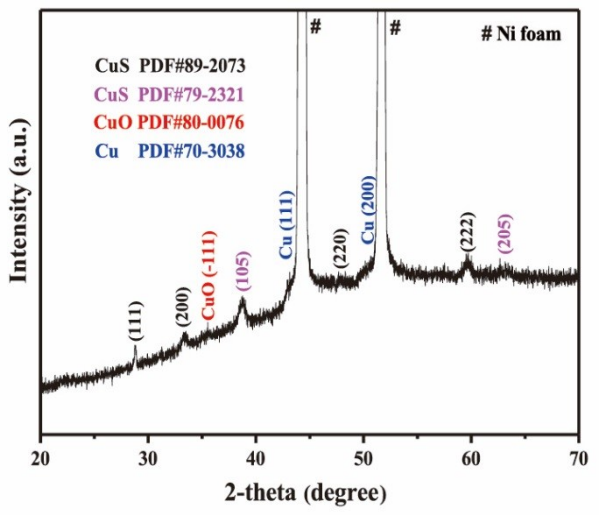

Figure S9 XRD pattern of CuS@NF after the 60-h CO_2 electroreduction.

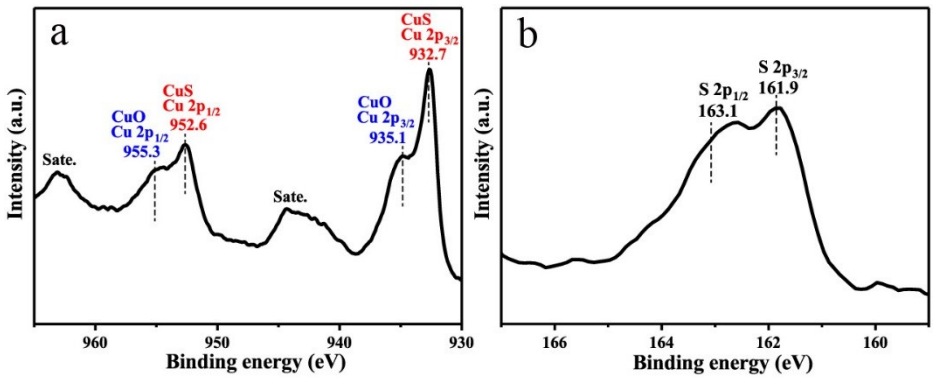

Figure S10 XPS spectra of CuS@NF after the 60-h CO_2 electroreduction. (a) Cu 2p; (b) S 2p.

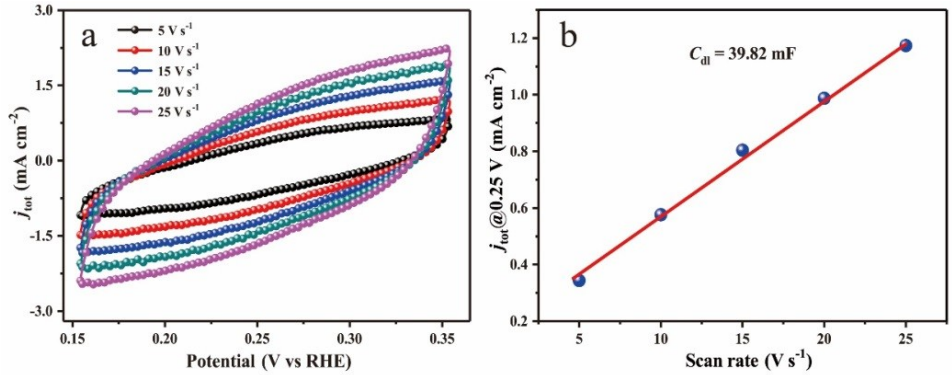

Figure S11 Determination of double-layer capacitance for the CuS@NF. (a) Cyclic voltammograms were measured in a non-faradaic region of the voltammogram at a sweep rate of 2, 4, 6, 8 and 10 mV/s; (b) The relationship between the current density and the scan rate.

Table S1 Comparison of CH_4 production in our study and previous literature.

Catalyst	**Electrolyte**	FE_{max} %	E_{max} V	**Ref.**
CuS@NF	0.1 M $KHCO_3$	73 ± 5	-1.1	This work
Melamine-treated carbon	0.1 M $KHCO_3$	0.75	-1.1	1
Copper electrode	0.5 M KCl	34(40 °C)	-	2
		71(10 °C)		
Cu_2O film@Cu	0.1 M $KHCO_3$	9.85	-0.99	3
Cu (100)	0.1 M $KHCO_3$	30.4		
Rh@Au (100)	-	40	-1.01	4
Rh@Ag (100)		10	-1.12	
Cu nanowire	0.1 M $KHCO_3$	55	-1.25	5
Ni_xGa_y	0.1 M $KHCO_3$	2	-0.48	6
Cu (100)	0.1 M $KClO_4$	30	-0.99	7
CuCl	0.1 M $KHCO_3$	1.47	-1.1	
Cu@GNNW@S	0.5 M $KHCO_3$	19	-1.4	8
Polypy coated Cu	CH_3OH/0.1 M $LiClO_4$	26	-3	9
Cu-polypyrrole	KOH/methanol	8	-3	10
Cu/Cu-L(0.025 M)	0.5 M KCl	26	-1.2	11
Cu/Cu-H(0.25 M)	0.5 M KCl	20	-1.2	
Cu foam	0.5 M $NaCO_3$	40	-1	12
Cu(2)PG/GC	0.1 M $NaHCO_3$	39	-1.3	13
Cu(2)GO/GC		44		
Cu(2)GC		13		
BAX	0.1 M $KHCO_3$	0.073	-0.8	14
CPS		0.041	-0.9	
CPSN		0.126	-1.2	
Cu	0.1 M $LiHCO_3$	6	-1.1	15
	0.1 M $NaHCO_3$	18		
	0.1 M $KHCO_3$	15		
	0.1 M $RbHCO_3$	13		
	0.1 M $CsHCO_3$	9		

Reference

1. W. Li, B. Herkt, M. Seredych and T. J. Bandosz, *Appl. Catal., B: Environ.*, 2017, **207**, 195–206.
2. H. Hashiba, S. Yotsuhashi, M. Deguchi and Y. Yamada, *ACS Comb. Sci.*, 2016, **18**, 203–208.
3. D. Ren, Y. L. Deng, A. D. Handoko, C. S. Chen, S. Malkhandi and B. S. Yeo, *ACS Catal.*, 2015, **5**, 2814–2821.
4. M.–J. Cheng, E. L. Clark, H. H. Pham, A. T. Bell and M. Head-Gordon, *ACS Catal.*, 2016, **6**, 7769–7777.
5. Y. Li, F. Cui, M. B. Ross, D. Kim, Y. Sun and P. Yang, *Nano Lett.*, 2017, **17**, 1312–1317.
6. D. A. Torelli, S. A. Francis, J. C. Crompton, A. Javier, J. R. Thompson, B. S. Brunschwig, M. P. Soriaga and N. S. Lewis, *ACS Catal.*, 2016, **6**, 2100–2104.
7. D. Ren, Y. Huang and B. S. Yeo, *Chimia (Aarau)*, 2015, **69**, 131–135.
8. Y. Wang, S. Fan, B. AlOtaibi, Y. Wang, L. Li and Z. Mi, *Chemistry*, 2016, **22**, 8809–8813.
9. R. Aydın, H. Ö. Doğan and F. Köleli, *Appl. Catal., B: Environ.*, 2013, **140–141**, 478–482.
10. S. Ohya, S. Kaneco, H. Katsumata, T. Suzuki and K. Ohta, *Catal. Today*, 2009, **148**, 329–334.
11. G. Keerthiga, B. Viswanathan and R. Chetty, *Catal. Today*, 2015, **245**, 68–73.
12. A. Dutta, M. Rahaman, N. C. Luedi, M. Mohos and P. Broekmann, *ACS Catal.*, 2016, **6**, 3804–3814.
13. Y. Lum, Y. Kwon, P. Lobaccaro, L. Chen, E. L. Clark, A. T. Bell and J. W. Ager, *ACS Catal.*, 2016, **6**, 202–209.
14. W. Li, M. Seredych, E. Rodriguez-Castellon and T. J. Bandosz, *ChemSusChem*, 2016, **9**, 606–616.
15. M. R. Singh, Y. Kwon, Y. Lum, J. W. Ager, 3rd and A. T. Bell, *J. Am. Chem. Soc.*, 2016, **138**, 13006–13012.